Proceedings of the Canadian Society for Mechanical Engineering International Congress
31st Annual Conference of the Computational Fluid Dynamics Society of Canada
CSME/CFD2024
May 26–29, 2024, Toronto, Ontario, Canada

CFD SIMULATION OF FAN-DRIVEN AIRFLOW IN A CLOSED ROOM

Peter Sharpe[1], Scott Simmons[2], Amir Aliabadi[3], William Lubitz[3]
[1]PhD Student, School of Engineering, University of Guelph, Guelph, Canada
[2]Postdoctoral Fellow, School of Engineering, University of Guelph, Guelph, Canada
[3]Associate Professor, School of Engineering, University of Guelph, Guelph, Canada

Abstract— Fan-driven air velocity in a closed, sealed room was measured using three-axis sonic anemometers and simulated with computational fluid dynamics (CFD) using a Reynold's Average Navier Stokes (RANS) *k-ε* turbulence methodology. The fan was fully contained within the room, and there was no meaningful air exchange into or out of the room. The measurements and simulations were conducted at a frequency of one hertz and averaged over a 30-minute period. Three grid resolutions were used in the simulation, with moderate improvements found with increasing resolution. The simulation results show close correlation with the experimental measurements, averaging less than seven percent error normalized to the average room inlet velocity. The methods used will be employed in future studies to enhance energy models for agricultural greenhouse environments.

Keywords-component; Airflow; Simulation; CFD; Turbulence

I. INTRODUCTION

The use of Computational Fluid Dynamics (CFD) techniques to model fan driven airflow in an enclosed room is of interest to the authors for the purpose of supplementing existing energy transfer models for agricultural greenhouses. An existing lumped capacitance heat transfer model performs well under most normal operating conditions. However, when horizonal curtains are used (for light abatement or heat containment) the model becomes less accurate [1], [2]. Also, the use of large fans to circulate air in greenhouses is becoming a normal practice, beneficial for regulating humidity and temperature levels and aiding in crop transpiration. For greenhouses using fans like this the existing energy transfer model is also less accurate. The purpose of this study was to gain knowledge in CFD modeling techniques that will be helpful to later supplement the existing greenhouse energy transfer model and improve its accuracy under these conditions.

Being able to control and predict how air flows in enclosed spaces is important in engineering applications and affects comfort and energy efficiency. The use of CFD to predict airflow in rooms is well covered in the literature. Studies have had success at accurately predicting airflow using Reynold's Averaged Navier Stokes (RANS) turbulence modeling with *k-ε* eddy viscosity model for the Reynold's stress term, where κ represents the turbulence intensity, and ε is the dissipation rate.

Bassiouny et al. successfully modeled a simple cuboid room with a ceiling fan using the RANS *k-ε* methodology and observed qualitatively that predicted air velocity magnitudes correlated well with data measured in a different study [3], [4]. They did not however quantify the error.

Chen et al. also used RANS with the standard *k-ε* model to successfully simulate fan airflow in a simple cuboid room. They found good correlation with experimental data for various fan geometries and rotational fan speeds. They also quantified the error with normalized root mean square deviation (NRSMD), where the root squared average difference of all sensor locations was divided by the total spread of simulated values [5], [6]. The reported maximum NRSMD was 19.3%.

Lin conducted a study of a ceiling mounted fan above an occupant seated at a desk [7], measuring the air velocity and temperature in a grid pattern between the fan and the occupant, and modeling using a *k-ε* based CFD simulation. The discrepancy between measured and simulated results was reported as 3.6%, though this compared overall magnitudes, and not individual velocity components.

Casseer and Ranasinghe compared four different turbulence models in analyzing fan driven airflow in an enclosed room [8]. They found that the NRMSD was 7.0% for the Spalart Almaras model, and 13.3% for the standard *k-ε* model. The other two models evaluated, Reynold's-normalization group *k-ε* and *k-ω*, resulted in NRMSD values over 23%.

This study is comprised of an experimental component, where velocity measurements of fan driven airflow were taken in an enclosed room of asymmetric geometry, and a computational component where CFD was used to model the airflow for comparison with the experimental measurements. The results are evaluated qualitatively with flow visualization tools and quantitatively with error calculations.

II. EXPERIMENTAL SETUP AND DATA COLLECTION

The room used in this study was a classroom at the University of Guelph, School of Engineering, measuring approximately 8.8 by 9.5 m. A picture of the fan and anemometers is shown in Fig. 1. An overview of the room geometry, fan position, and sensor locations is shown in Fig. 2. The fan assembly was positioned in the center of the room, and all openings of the room were closed or sealed, including

ventilation ducts. The experiment took place during spring in Canada, and there was no internal heating present. On the window side of the room the blinds were drawn during the experiments to minimize solar radiation heating effects from outside. Airflow was generated using a 30 inch diameter two blade axial flow fan made by the Patterson Fan Company intended for air circulation in industrial settings. The motor turning the fan blades had a rating of one horsepower, 115 volts alternating current motor, with a full load amperage (FLA) of 13.4 amps, made by Marathon Electric. Air from the fan outlet passed through a 1.2 m -long square duct measuring approximately 0.8 m wide by 0.8 m tall. At the end of the duct was a diffuser plate with a grid of nested holes measuring approximately four millimeters in diameter (see Fig 2 inset).

Figure 1. Fan positioned in room and sonic anemometers

The velocity of the air exiting the duct through the diffuser plate was surveyed using a pitot probe sensor, positioned 70 mm downstream of the plate at evenly spaced locations over a five-by-five grid pattern. Twenty-five measurements were taken at a 1 Hz sample rate at each grid location for one- minute intervals. The average exit velocity over the grid was 8.07 m/s with a standard deviation of 0.66 m/s. This corresponds to an average exit flow rate of 13.5 m^3/s (2650 cfm).

Air velocity measurements in the room were taken at prescribed locations using three three-axis sonic anemometers (RM Young model 8100). Five runs were completed, with the probes moving to a new location for each run, totaling fifteen measurement locations. Each run lasted one hour, and the middle 30 minutes of data were averaged for comparison with the CFD simulation results. The center of the anemometers' sensing volumes were set at the height of the fan rotation axis (1.321 m) for all tests. In addition to air velocity, the sensors also measured air temperature. All measurements were recorded by Campbell Scientific CR-1000 dataloggers at a sample rate of 1 Hz.

I. CFD SIMULATIONS

As in previous studies ([3], [6], CFD simulations were made using a RANS based *k-ε* turbulence method. The tool used for simulations was OpenFOAM version 8 (www.openfoam.com), with the simpleFoam solver. A solid model of the room was generated using SolidWorks CAD software (see Fig. 4), and then used to create the mesh with blockMesh and snappyHexMesh. Three different grid resolution levels were tried; coarse, medium, and fine. The snappyHexMesh mesh refinement setting was set to 3, meaning each boundary cell was divided into three segments in each direction, yielding nine boundary cells for each interior cell. The finest mesh level yielded marginally more accurate results as shown in Fig. 3. A view of the coarse and medium grid resolutions is shown in Fig. 4. The effect of grid size on the output is shown in Fig. 7, where the time history of the simulation shows much less variation with the finer grid.

The fan was treated as a simple cuboid with the outlet face (room inlet) given a uniform velocity field matching the average surveyed value of 8.07 m/s. The fan inlet face (room outlet) was treated as a zero-pressure gradient condition. All other surfaces in the room were treated as no slip walls. The turbulence intensity factor *k* was set to 0.25, which is approximately equal to the average value for sensors B1, C2, C3 and C5. These sensors were chosen for approximating *k* because they were in areas of high flow where the mean value is not close to zero. Values of *k* are the ratio of the standard deviation to the mean value:

$$\kappa = \sigma / \mu \qquad (1)$$

The numerical simulations were conducted using the parallel computing server network housed by the University of Guelph's Atmospheric and Innovations Research (AIR) Laboratory. Thirty parallel processors were used for each simulation. The largest simulation required approximately three hours to run. Grid resolutions with cell counts above 7×10^6 were attempted but failed. More investigation is needed to determine the cause of these failed runs.

Figure 2. Fan oulet diffuser grid with pitot probe

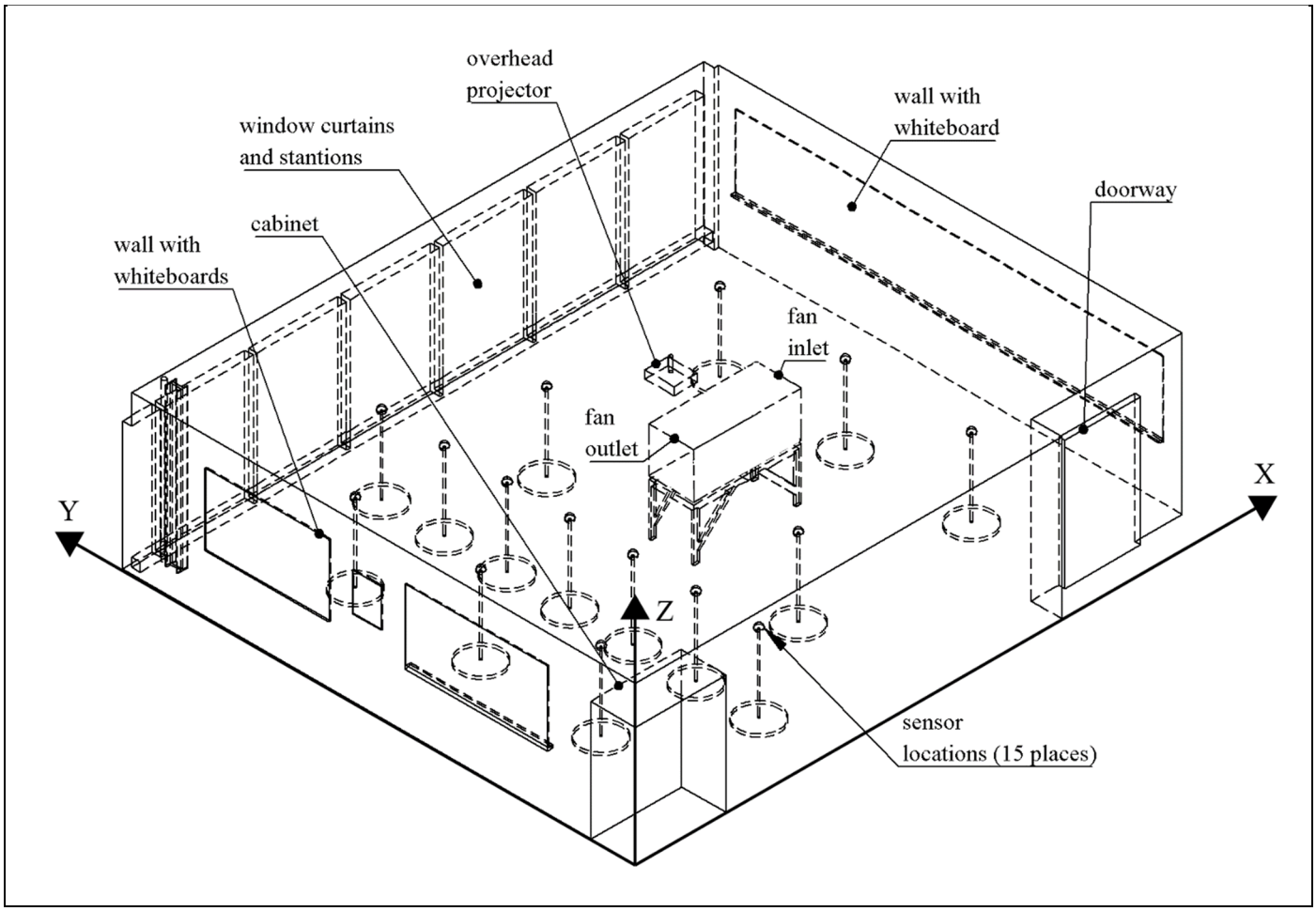

Figure 3. CAD model of room showing wall geometry, fan and sensor locations.

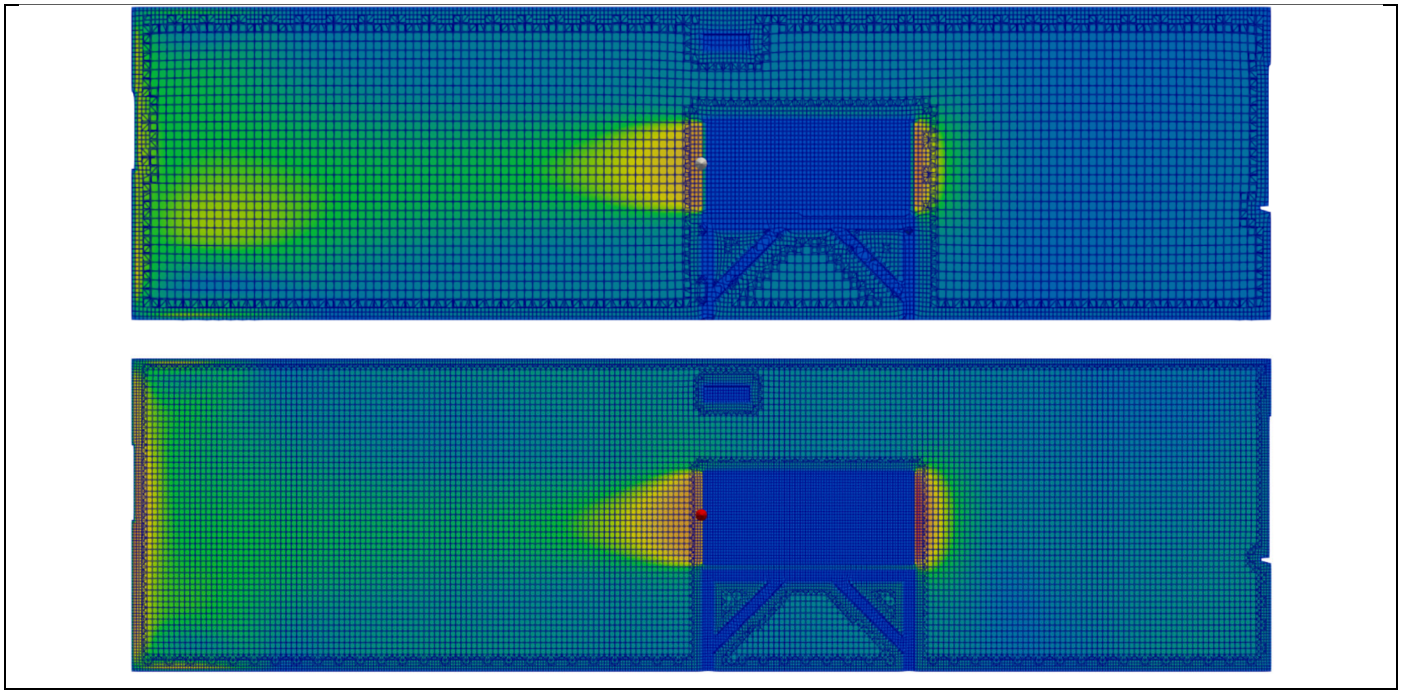

Figure 4. XZ plane showing coarse (top) and medium (bottom) grid resolutions

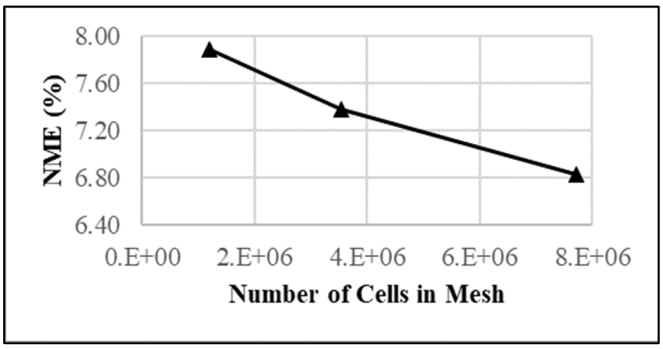

Figure 5. Grid convergence

II. RESULTS AND DISCUSSION

Only results of the finest grid simulation are presented here. For the simulation (prediction) and measurements (observation), unless otherwise mentioned, the data was averaged over the middle thirty minutes of a one-hour time span. The comparison of observed and predicted air velocity is presented subjectively with a quiver plot showing the X and Y velocity components (U and V) in the horizontal plane (Fig 6), and objectively with quantified error calculations, summarized in Table 1.

Velocity components in the horizontal plane are the focus as the vertical component was small with the least variation. This trend can be seen in the time history graph of the simulation for all fifteen sensor locations (Fig 7). It shows that after approximately 10 minutes variation is minimized, though the solution for the sensors immediately in the fan wake converges to approximately -8 m/s much quicker than that. It can also be seen from this time history that the variation for these two sensors is minor compared with the others.

A. Qualitative Comparison

The quiver plot (Fig. 6) shows that the simulation performed well at predicting the flow pattern. The bold arrows represent the average predicted and average measured velocities U and V for the thirty-minute period between fifteen and forty-five minutes. The background colour plot, enhanced with scaled line segment glyphs is taken from the simulation at time equals thirty minutes. The directions and magnitudes are correlated at the sensor locations.

The simulation colour plot shows two primary flow patterns after the fan stream is divided by the west wall. A portion is diverted north and tends to recirculate back to the fan outlet stream. The rest is diverted south towards the cabinet and sets up a recirculation pattern back to the fan inlet. A portion of this south recirculation pattern continues to the northeast corner of the room and before turning back to the northwest recirculation path. Lastly, the simulation shows that the air moving to the inlet comes primarily from the south recirculation path. Fig. 6 also shows close directional agreement, but poor magnitude correlation for the two sensors immediately downstream of the fan outlet. This discrepancy is discussed further in the next section.

B. Quantitative Comparison

The difference between predicted and observed values is quantified in three ways; normalized mean error (NME), simple bias (B), and root square mean error (RSME) These values are calculated by equations 2-4, where Φ represents the velocity component U, V or W. The denominator used in the NME is taken as the average velocity at the fan outlet (8.07 m/s). NSME is a similar measure to that used in [4], where the denominator was the total variance of observed values. B and RSME are recommended in [9] for a quantitative method evaluation. Other means of quantifying error, such as fractional bias (FB) and normalized mean square error (NMSE), also recommended in [9], are not meaningful in this scenario because the average velocities for most of the sensors are near zero [9].

$$NME = (\Phi_P - \Phi_O)/8.07 \quad (2)$$

$$B = \Phi_P - \Phi_O \quad (3)$$

$$RSME = ((\Phi_P - \Phi_O)^2)^{(1/2)} \quad (4)$$

The average error values for all fifteen sensors are summarized in Table 1. A more detailed summary, showing average data for each of the fifteen sensors is presented in the Appendix. The main source of bias error comes from the U component, which was dominated by the sensors immediately in the wake of the fan outlet (sensors B1 and C3), where there was decent directional correlation, but poor magnitude agreement. This could be due to oversimplification of how the fan outlet velocity was modeled: a uniform one directional square of airflow. While the diffuser plate is effective in directing the flow, it is likely there is more multi-directionality to the actual output flow. Error measures NME and RSME showed comparable results, which is not surprising as they are both calculated in similarly. The lowest error was for the vertical velocity component (W), followed by the fan-aligned component (U), and lastly the fan-orthogonal component (V).

When the error values are averaged across the three velocity components, the values are 6.65 %, -0.14 m/s and 0.54 m/s for NME, B and RSME. These overall values of error indicate the predictions are well aligned with the measurements, and that the model can be used for predicting the observed velocities under the prescribed conditions.

The error results are of similar magnitude as those reported in [6] - [8]. Chen et al. reported a maximum NRSME of 19.3%, where the maximum found in this study was 22.3%. Lin found an overall average magnitude error of 3.6%, and Casseer and Ranasinghe reported the average NRSMD to be 13.3%. This study found the average NME to be 6.65%.

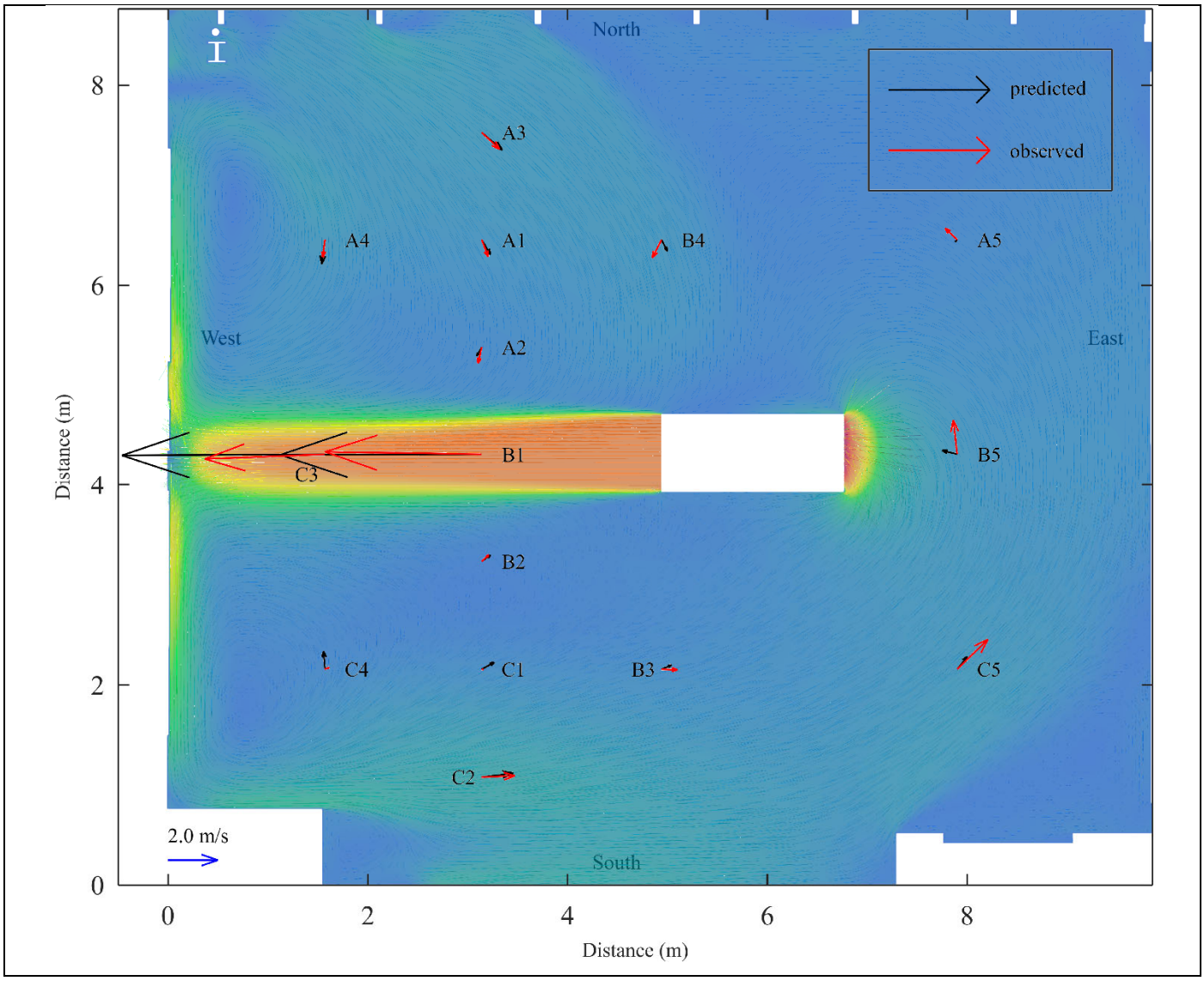

Figure 6. Quiver plotsof observed and predicted results in XY plane overlaid on velocity magnitude plot at thirty minutes

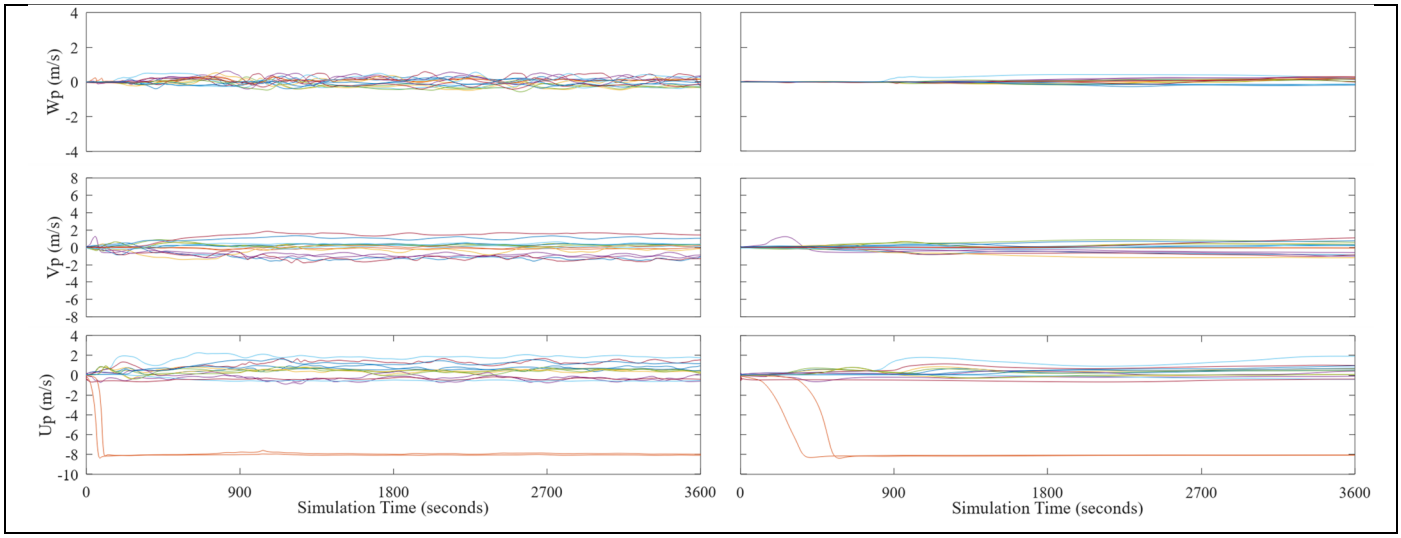

Figure 7. Time history plot of simulation for all fifteen sensor locations, coarse grid (left), fine grid (right)

TABLE I. AVERAGE ERROR FOR ALL SENSOR LOCATIONS

	predicted (m/s)	observed (m/s)	NME (%)	B (m/s)	RSME (m/s)
U	-0.862	-0.509	7.22	-0.353	0.58
V	-0.065	0.008	10.2	-0.074	0.82
W	0.011	0.014	2.51	-0.003	0.20
		average	6.65	-0.14	0.54

III. CONCLUSIONS

The RANS k-ε CFD simulation method successfully predicted the measured fan driven air velocities in a closed room. The overall average normalized mean error (NME) was less than 10%, and the average root mean square error was less than 0.6 m/s. The CFD simulation provided insight into the overall flow patterns that cannot otherwise be determined without significant measurement and analysis. The method was employed with relative ease and will form the foundation for future simulations in agricultural greenhouse environments.

ACKNOWLEDGMENT

This work was completed as part of a larger study funded by the Ontario Ministry of Agriculture, Food and Rural Affairs (OMAFRA) Agrifood Innovation Alliance Tier 1 program: "UG-T1-2022-101640: Performance of vertical and through-curtain greenhouse fans in the presence of light abatement curtains".

REFERENCES

[1] A. Nauta, J. Han, S. H. Tasnim, and W. D. Lubitz, "Performance Evaluation of a Commercial Greenhouse in Canada Using Dehumidification Technologies and LED Lighting: A Modeling Study," *Energies (Basel)*, vol. 16, no. 3, Feb. 2023, doi: 10.3390/en16031015.

[2] A. Nauta, S. H. Tasnim, and W. D. Lubitz, "Simulation of an Earth-Air Heat Exchanger in a Commercial Greenhouse to Improve Energy Efficiency," *Journal of Biosystems Engineering*, 2023, doi: 10.1007/s42853-023-00188-8.

[3] R. Bassiouny and N. S. Korah, "Studying the features of air flow induced by a room ceiling-fan," *Energy Build*, vol. 43, no. 8, pp. 1913–1918, Aug. 2011, doi: 10.1016/j.enbuild.2011.03.034.

[4] A. Jain, R. R. Upadhyay, S. Chandra, M. Saini, and S. Kale, "Experimental Investigation of the Flow Field of a Ceiling Fan," in *Volume 3*, ASMEDC, Jan. 2004, pp. 93–99. doi: 10.1115/HT-FED2004-56226.

[5] Y. Gao *et al.*, "Ceiling fan air speeds around desks and office partitions," *Build Environ*, vol. 124, pp. 412–440, Nov. 2017, doi: 10.1016/j.buildenv.2017.08.029.

[6] W. Chen *et al.*, "Experimental and numerical investigations of indoor air movement distribution with an office ceiling fan," *Build Environ*, vol. 130, pp. 14–26, Feb. 2018, doi: 10.1016/j.buildenv.2017.12.016.

[7] H. H. Lin, "Improvement of human thermal comfort by optimizing the airflow induced by a ceiling fan," *Sustainability (Switzerland)*, vol. 11, no. 12, 2019, doi: 10.3390/SU11123370.

[8] D. Casseer and C. Ranasinghe, "Assessment of Spallart Almaras Turbulence Model for Numerical Evaluation of Ceiling Fan Performance."

[9] A. A. Aliabadi, "Model Evaluation," in *Turbulence: A Fundamental Approach for Scientists and Engineers*, Cham: Springer International Publishing, 2022, pp. 251–258. doi: 10.1007/978-3-030-95411-6_19.

APPENDIX

TABLE II. RESULTS AND ERROR SUMMARY FOR EACH SENSOR LOCATION

Position			U mean air velocity					V mean air velocity					W mean air velocity				
sensor	x	y	U_P	U_O	NME	B	RSME	V_P	V_O	NME	B	RSME	W_P	W_O	NME	B	RSME
-	(m)	(m)	(m/s)	(m/s)	(%)	(m/s)	(m/s)	(m/s)	(m/s)	(%)	(m/s)	(m/s)	(m/s)	(m/s)	(%)	(m/s)	(m/s)
A1	3.14	6.46	0.35	0.26	1.10	0.09	0.09	-0.60	0.68	15.9	-1.28	1.28	0.01	-0.08	1.11	0.09	0.09
B1	3.14	4.31	-8.07	-6.28	22.30	-1.80	1.80	-0.02	-0.10	0.94	0.08	0.08	0.01	0.38	4.53	-0.37	0.37
C1	3.14	2.16	0.51	0.06	5.54	0.45	0.45	0.28	0.01	3.43	0.28	0.28	-0.07	0.04	1.41	-0.11	0.11
A1	3.14	5.38	-0.20	-0.15	0.58	-0.05	0.05	-0.35	0.65	12.4	-1.00	1.00	0.12	-0.08	2.46	0.20	0.20
B2	3.14	3.23	0.36	0.28	0.89	0.07	0.07	0.25	-0.26	6.35	0.51	0.51	-0.10	0.28	4.70	-0.38	0.38
C2	3.14	1.08	1.26	1.33	0.87	-0.07	0.07	0.16	-0.05	2.63	0.21	0.21	0.37	-0.17	6.65	0.54	0.54
A3	3.14	7.53	0.83	0.71	1.40	0.11	0.11	-0.70	0.67	17.0	-1.38	1.38	0.04	-0.10	1.67	0.13	0.13
B3	4.94	2.16	0.40	0.64	2.92	-0.24	0.24	0.17	0.02	1.88	0.15	0.15	-0.14	0.07	2.56	-0.21	0.21
C3	1.57	4.31	-8.13	-4.81	41.1	-3.32	3.32	-0.05	0.19	2.90	-0.23	0.23	0.02	0.26	2.96	-0.24	0.24
A4	1.57	6.46	-0.13	-0.08	0.58	-0.05	0.05	-0.97	0.70	20.7	-1.67	1.67	-0.07	-0.02	0.64	-0.05	0.05
B4	4.94	6.46	0.23	-0.37	7.43	0.60	0.60	-0.46	0.72	14.6	-1.18	1.18	0.09	0.06	0.41	0.03	0.03
C4	1.57	2.16	-0.05	0.18	2.85	-0.23	0.23	0.72	-0.08	10.0	0.80	0.80	0.08	-0.19	3.35	0.27	0.27
A5	7.90	6.46	-0.08	-0.48	4.96	0.40	0.40	-0.08	-0.46	4.68	0.38	0.38	-0.07	-0.08	0.11	0.01	0.01
B5	7.90	4.31	-0.60	-0.16	5.50	-0.44	0.44	0.15	-1.36	18.8	1.51	1.51	-0.04	-0.26	2.79	0.23	0.23
C5	7.90	2.16	0.40	1.23	10.27	-0.83	0.83	0.51	-1.19	21.2	1.71	1.71	-0.10	0.09	2.37	-0.19	0.19
mean	4.02	4.31	-0.86	-0.51	7.22	-0.35	0.58	-0.07	0.01	10.2	-0.07	0.82	0.01	0.01	2.51	0.00	0.20